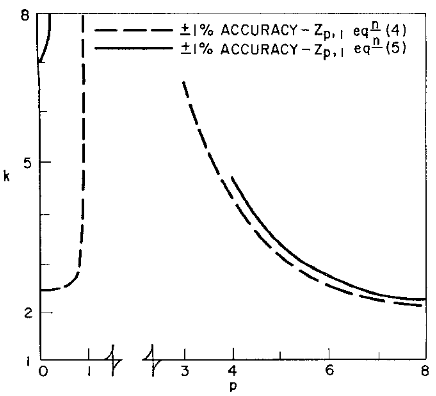

Fig. 1—Accuracy graph of the approximate formulas for $z_{p,s}$ with $s=1$.

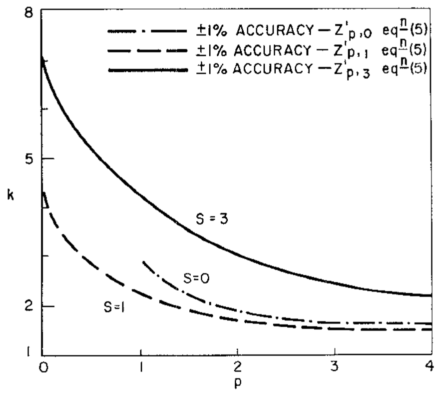

Fig. 2—Accuracy graph of the approximate formula for $z_{p,s}'$ with $s=0$, 1, and 3.

Setting $S=1$ in (4) gives Gunston's result.

It is known, though, that for given p, the roots of (1) and (2) do not coincide so it would be helpful if our simple formulas exhibited this difference. Using the full right-hand side of (3) above does yield dissimilar, but rather complex, results. By retaining only the most essential terms, however, these expressions can be approximately reduced to

$$z_{p,S} \approx \sqrt{\frac{(S\pi)^2}{(k-1)^2} + \frac{4p^2-1}{(k+1)^2}}$$

$$z'_{p,S} \approx \sqrt{\frac{(S\pi)^2}{(k-1)^2} + \frac{4p^2+3}{(k+1)^2}}$$

$$(S = 1, 2, 3, \cdots)$$

$$z'_{p,0} \approx \frac{2p}{(k+1)}\left[\frac{1+(k-1)^2}{6(k+1)^2}\right]. \quad (5)$$

For large S or small $(k-1)$ these formulas give rise to the leading terms in the asymptotic expansions of McMahon and Buchholz, and consequently the expressions of (5) become increasingly more accurate in these regions.

Following Gunston, accuracy graphs may be roughly constructed for the above simple approximate formulas. For values of (k, p) lying below the curves of Fig. 1 the formulas of (4) and (5) for $z_{p,1}$ are within ± 1 per cent of the exact value. Fig. 2 shows similar curves for $z'_{p,0}$, $z'_{p,1}$, and $z'_{p,3}$ from (5).

It is unfortunate that known existing data (see Waldron[5] and Fletcher, *et al.*[8]) does not permit us to readily compare *carefully* the approximate with the exact roots for a wider range of values of (k, p). In particular, the precise general accuracy of the expressions for $z_{p,S}$ of either (4) or (5) is somewhat uncertain for moderate p and k, say $1<p<3$ and $k>3$, and the situation is therefore not quite as depicted in Fig. 1 of Gunston.[1,9] Nevertheless, it is hoped that the two figures presented here do serve to illustrate the general regions of applicability of the formulas of (4) and (5) as either reasonable approximate values of the roots in question, or as initial approximations in computational schemes for the zeros of these important combinations of Bessel functions.

J. A. Cochran
Bell Telephone Labs., Inc.
Whippany, N. J.

[8] A. Fletcher, *et al.*, "An Index of Mathematical Tables," Addison-Wesley, Reading, Mass., 2nd ed., vol. 1, pp. 413, 414, 416; 1962.

[9] For instance, the inaccuracy of Gunston's formula for $p=5/2$, $k=3, 4$, or 5 is of the order of 2 or 3 per cent rather than less than 1.5 per cent as his figure indicates.

Transmission Line Measurement of Narrow Linewidth Ferromagnetic Samples*

Measurement of ferromagnetic resonance linewidths over a range of microwave frequencies is facilitated by the use of a nonresonant waveguide system. The loading effect encountered in such a transmission line system, however, becomes significant when the linewidth is less than a few tens of oersteds. The effect of transmission line loading was avoided by the use of an automatic compensation network.

An idealized model of the experimental system is illustrated in Fig. 1. Scattering-matrix theory is applied to the junction that is inside the balloon-like simply connected region. The test sample is placed topologically outside the junction by means of a connecting tube. If the radius of the connecting tube is small enough, the tube itself will not be significant and we have a three-port function which fits the usual simplifying assumptions of scattering matrix theory. Ports Nos. 1 and 2 are terminals of waveguide in which only the dominant mode is propagating. Port No. 3 is the surface which

* Received July 1, 1963.

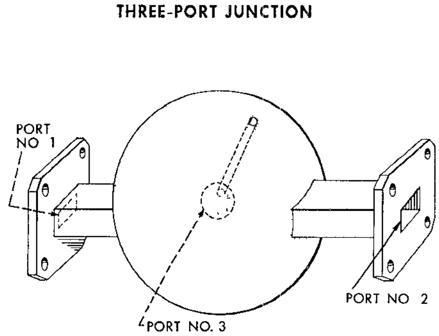

Fig. 1—Schematic view of the test section.

surrounds the test sample. The treatment of this problem is simplified by including only one mode of propagation at port No. 3. This propagating mode is closely related to the radiation field associated with the resonant mode of the sample.

It is necessary to consider the properties of the test section in terms of the signals observable at ports Nos. 1 and 2 alone. The only dissipative element in this system is the load at port No. 3. The reflection coefficient of the load at port No. 3 is written in impedance form for convenience, $(1-z)/(1+z)$. If first order perturbation theory can be used to describe a magnetic sample in the waveguide the impedance is proportional to the susceptibility.

In order to describe this three-port junction in matrix formalism, it is sufficient to identify the ports with elements of a column matrix, the amplitude and phase at each port being represented by a corresponding element. The scattered waves, also described by a column matrix, are related to the incident waves by a square matrix. Terminating the third port of the network by a reflective load reduces the order of system. The resultant two-port junction is described by a 2×2 matrix T, given in (1), which is not, in general, a unitary matrix.

$$T = \begin{bmatrix} \dfrac{(s_{11}-s_{22}^*)+(s_{11}+s_{22}^*)z}{(1-s_{33})+(1+s_{33})z} & \dfrac{(s_{12}+s_{21}^*)+(s_{12}-s_{21}^*)z}{(1-s_{33})+(1+s_{33})z} \\ \dfrac{(s_{21}+s_{12}^*)+(s_{21}-s_{12}^*)z}{(1-s_{33})+(1+s_{33})z} & \dfrac{(s_{22}-s_{11}^*)+(s_{22}+s_{11}^*)z}{(1-s_{33})+(1+s_{33})z} \end{bmatrix}. \quad (1)$$

The impedance at the third port appears in the reduced matrix T in the numerator of each term and in the common denominator of the entire matrix. A resonant condition is described by this matrix if the denominator vanishes. This, however, represents decoupling of the third port from all other ports and is of no interest in this study. The complex conjugate form arises because S is a unitary matrix; the form written here is for $+1$ value of the determinant of S.

It is useful to note at this point that: 1) Since signal is applied at one port only, the transmitted and reflected signals are the most easily observed quantities. 2) Since the sample has a narrow linewidth, the condition $z=0$ can be used for a convenient reference, the measurement being made far from resonance.

The measured amplitudes of the reflected and transmitted signals are proportional to the amplitude of the matrix elements in the first column of the matrix. Linear combination of the incident and reflected signals in a bridge circuit makes it possible to generate a signal with similar form for which the values of the constants are adjustable. If the bridge is balanced off resonance, that is with $z=0$, the constant in the numerator drops out.

The term $(1+s_{33})$ in the denominator represents the observed line broadening associated with the radiation of energy from the sample. If the $(1+s_{33})$ term is not negligible, the observations of linewidth are made difficult by the influence of the coupling of the sample to the waveguide. It is possible for the coupling to be large enough to make precision linewidth measurements a practical impossibility. One method of eliminating this difficulty is to use the transmitted signal as the reference throughout the experiment. This can be accomplished by appropriately adjusting the incident amplitude. The reflected signal R is the ratio of the terms in the first column of the matrix (1).

$$R = \frac{(s_{11} - s_{22}^*) + (s_{11} + s_{22}^*)z}{(s_{21} + s_{12}^*) + (s_{21} - s_{12}^*)z}. \qquad (2)$$

The constant, $(s_{11}-s_{22}^*)$, in the numerator drops out when the bridge is balanced far off resonance since R must then be zero. The denominator term $(s_{21}-s_{12}^*)$ is of special interest since this term vanishes if two restrictions are applied to the original S matrix. The first is that the matrix be symmetric. This is easily fulfilled and tested physically since this is identical to the requirement of reciprocal coupling. It is possible to test this in a magnetic resonance experiment by reversing the magnetic field and observing the reciprocity of the resonant properties.

The other condition requires that the three-port matrix S be one in which, by adjusting only the phase reference at the external ports, it is possible simultaneously to obtain real, positive values for both the determinant of the S matrix and the matrix component s_{21}. In a physical analysis, this is equivalent to the removal of wall effects, or to the condition that there is no shift of the resonant frequency due to coupling of the waveguide system. A frequency shift can be associated with a reaction loading by the transmission line. Only if the *reactive* loading is kept small will we be able to compensate for the *resistive* loading effect by the waveguide system.

$$R = \frac{s_{11} + s_{22}^*}{s_{21} + s_{12}^*} z. \qquad (3)$$

The final form of the reflected signal (3) is obtained by applying these requirements; the system is reciprocally coupled, the bridge is balanced off resonance so that $z=0$, the transmitted signal is held constant, and the sample is not located near the waveguide wall. Since R is proportional to z, the observed linewidth of R is likewise the intrinsic linewidth of the sample.

The dependence of the apparent linewidth upon an error in satisfying the reciprocity condition was tested experimentally. The linewidth of the reflected signal *did* vary somewhat with change in position of the sample in the waveguide; however, there was no *pronounced* sensitivity in the observed linewidth. The precision to which the reciprocity condition could be satisfied was sufficient to warrant use of this system. The final system error was much greater than the residual error associated with position error.

The microwave bridge circuit used to observe the resonance linewidth is shown in Fig. 2. The klystron stabilization held the signal frequency to a preset value with only a small residual frequency modulation. The reference and reflection signal branches were coupled to the main branch through 10-db and 3-db directional couplers, respectively, and were mixed for bridge operation in the 3-db coupler. The modulation servo-amplifier allowed for automatic compensation for transmission line loading upon the resonant sample. The test section shown in Fig. 3 was constructed of RG 52/U waveguide.

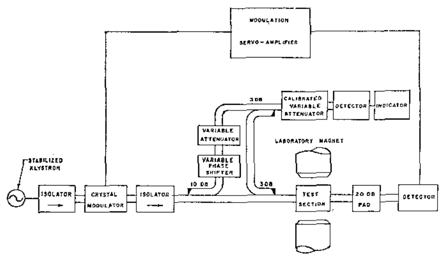

Fig. 2—Block diagram of the measurement system.

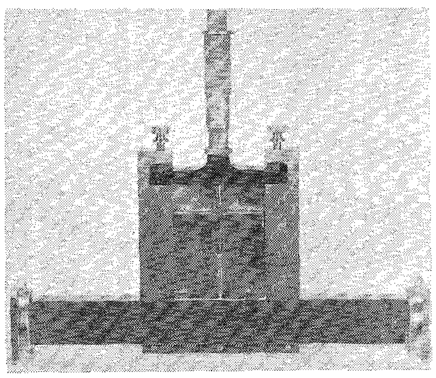

Fig. 3—Photograph of the test section with sample holder in place.

The reflection bridge was balanced by adjustment of the phase shift and attenuation on the reference arm. Measurements were made by observing the magnetic field difference corresponding to the 3-db response width of the reflection bridge signal. The magnetic field was measured with suitable precision using a nuclear magnetic resonance gaussmeter and a frequency counter for narrow linewidths. For narrow linewidths the final precision was ± 0.02 oersted.

George R. Jones
Harry Diamond Lab.
Washington, D. C.

A Note on Strip-Line Band-Stop Filters with Narrow Stop Bands*

Design criteria for band-stop filters having bandwidths up to few per cent have been presented by Young, Matthaei, and Jones. The purpose of this correspondence is to extend their work to include a new type of strip-line resonator which is easier to construct and adjust, and also permits the application of printed circuit fabrication.

Fig. 1 shows the basic structure of the band-stop filter to be considered corresponding to Fig. (3a) of the paper by Young, *et al.*[1] Fig. 2 shows a schematic of how the circuit of Fig. 1 may be realized in practice corresponding to Fig. 5 of the cited reference. However, resonant circuits of the type shown require considerable care in adjustment as noted by the design example given by Young, *et al.* The major difficulties are in determining the gap spacing required to obtain the proper value of resonator capacitance and in establishing the reference planes for the stub lengths. The type of resonator shown in Fig. 3 and which is the subject of this note will eliminate these difficulties. The only adjustment required is the position of the short circuit which is made necessary to compensate for the mitered corners. Only the case where all transmission lines have equal characteristic impedances is considered. This limits the design criteria to applications where a maximum flat response or Tchebyscheff response with an odd number of resonators is desired. The extension to the general case is readily accomplished, but will not be considered here.

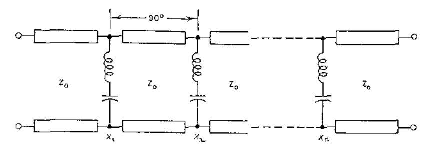

Fig. 1—Quarter wave coupled shunt resonator band-stop filter.

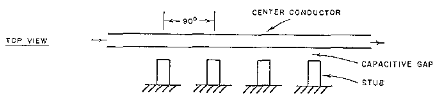

Fig. 2—Physical center conductor geometry for strip-line filter.

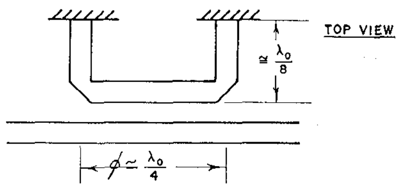

Fig. 3—Parallel coupled line resonator.

* Received July 17, 1963. Based on part of the research work undertaken by Robert Dean Standley in partial fulfillment of the requirements for the Ph.D. degree at Illinois Institute of Technology, Chicago, Ill.

[1] L. Young, *et al.*, "Microwave band-stop filters with narrow stop bands," IEEE Trans. on Microwave Theory and Techniques, vol. MTT-10, pp. 416–428; November, 1962.